Polymer 51 (2010) 1632–1638

Contents lists available at ScienceDirect

Polymer

journal homepage: www.elsevier.com/locate/polymer

# Determination of lamellar twisting manner in a banded spherulite with scanning microbeam X-ray scattering

Tatsuya Kikuzuki [a,*], Yuya Shinohara [a,*], Yoshinobu Nozue [b], Kazuki Ito [c], Yoshiyuki Amemiya [a]

[a] Graduate School of Frontier Sciences, The University of Tokyo, 5-1-5 Kashiwanoha, Kashiwa, Chiba 277-8561, Japan
[b] Petrochemicals Rsearch Laboratory, Sumitomo Chemical Co. Ltd., Kitasode, Chiba, Japan
[c] RIKEN, Harima Institute, SPring-8, 1-1-1 Kouto, Sayo, Hyogo 679-5198, Japan

ARTICLE INFO

*Article history:*
Received 27 October 2009
Received in revised form
18 January 2010
Accepted 25 January 2010
Available online 2 February 2010

*Keywords:*
A banded spherulite
Scanning microbeam X-ray diffraction
Lamellar twisting

ABSTRACT

We investigated lamellar twisting manner in a banded spherulite, the blend of poly-(ε-caprolactone) and poly-(vinyl butyral), with scanning microbeam X-ray diffraction. We obtained the diffraction contour intensity map with a scanning pitch of 1 μm by employing a rotation of a spherulite around its radial direction along which the microbeam scans. The results confirm that the twisting manner depends on the crystallization temperature and that it changes from continuous twisting to step-wise twisting with the increase of crystallization temperature. Moreover, we observed that the phase of long-period lamellar twisting advanced by about 15° compared to that of short-period lamella. In addition, it was confirmed that *c*-axis of packing structure was normal to lamella, which was represented by dominant short-period lamella.



## 1. Introduction

Many polymer blend systems show micron-scale inhomogeneity in their structures. Such micron-scale inhomogeneity influences the physical properties of systems such as toughness [1], electric conductivity [2], and viscoelasitc property [3]; hence deep understanding of the inhomogeneity is important to elucidate the relationship between properties and structure. Since the pioneering work by Point [4], Keith and Padden [5], Keller [6], Price [7], and Gathercole [8], periodic banding in polymer spherulites examined in polarized optical microscope has attracted large attention. The origin of the banding is attributed to the twisting of lamella, although there remain controversial discussions about the origin of lamellar twisting [9–13]. Calculation of scattering profiles from twisting lamella was also performed [14]. Among a number of banded spherulites, we have focused on the blend of poly-(ε-caprolactone) (PCL) and poly-(vinyl butyral) (PVB), which forms a banded spherulite. By adding a small amount of PVB to PCL, the nucleation rate of PCL is suppressed by two orders of magnitude and PCL forms highly ordered banded spherulites, resulting in the formation of large banded spherulites, while no banded PCL spherulite grows without PVB.

In order to investigate the detailed structural inhomogeneity which appears in the banded spherulites, we used scanning microbeam small-angle X-ray scattering (SAXS) and wide-angle X-ray diffraction (WAXD), which has been successfully applied for the investigation of the spatial distribution of nano- and subnano-structure in micron-scale [15–19]. The pitch of banding in PCL/PVB spherulites depends on crystallization temperature and is around 10–20 μm. The lamellar twisting manner can be, therefore, investigated in detail with an X-ray microbeam of μm scale. For example, the microbeam WAXD clearly showed the handedness of lamellar twisting in a spherulite [20]. Furthermore, we previously reported that lamellar twisting manner in PCL/PVB depended on the crystallization temperature by using scanning X-ray microbeam: lamella in a spherulite crystallized at 41 °C showed a step-wise twisting while a uniform twisting was observed for lamella in a spherulite crystallized at 35 °C [21]. We have noticed, however, that the previous analyses contained some uncertainty in determining the twisting manner (in Section 3.1.3). In this paper, we propose a method which allows us to determine the twisting manner without ambiguity. In this method, the rotation of sample has been introduced to scanning microbeam X-ray scattering. The rotation of sample was already introduced to polarized optical microscope (POM) [4,6,8], and therefore, the present POM technique also enables us to observe the twisting manner of lamella

* Corresponding authors.
*E-mail addresses:* kikuzuki@issp.u-tokyo.ac.jp (T. Kikuzuki), yuya@k.u-tokyo.ac.jp (Y. Shinohara).

0032-3861/$ – see front matter © 2010 Elsevier Ltd. All rights reserved.
doi:10.1016/j.polymer.2010.01.057

without ambiguity with a spatial resolution of 100 nm. However, with POM, it is impossible to observe it in relation to the twisting manners of main lamella, secondary lamella and packing structures. In this paper, we show that we can observe not only stepwise twisting of main lamella but also that of secondary lamella and packing structure. Furthermore, phase shift between these twisting manners can be observed with scanning microbeam X-ray scattering in combination with the sample rotation.

## 2. Materials and methods

### 2.1. PCL/PVB blend spherulite

We prepared a two-dimensional spherulite of PCL/PVB blend, the thickness of which was 70–90 μm. PCL and PVB were supplied by Wako Chemicals ltd. and were used as received. Molecular weight of PCL and PVB were 40,000 and 100,000, respectively. The PCL/PVB blend sample was prepared by dissolving a desired ratio of PCL to PVB in tetrahydrofuran, which was common solvent. The PCL/PVB blend ratio used in this experiment is 95/5. The solution sample was cast upon a glass plate. We put this plate into a draft until the solvent is removed at room temperature. Then a small amount of blend film was cut from the glass plate and was put on a sheet of thin mica that was placed on a temperature-controlled stage (LINKAM THMS-600). After the sample melted, we put another sheet of thin mica on this sample to make it to be flat. The thickness of the sample was 70–90 μm. The sample was kept at 90 °C for 15 min and then it was quenched and isothermally crystallized at 39 °C (PCL/PVB39), 45 °C (PCL/PVB45), or 48 °C (PCL/PVB48). Images taken with polarized optical microscope are shown in Fig. 1. Crystallized temperatures in Fig. 1 are 39 °C, 42 °C, 45 °C. The size of spherulites becomes larger and the crystallinity apparently becomes better with higher $T_c$.

### 2.2. Scanning microbeam wide-angle X-ray diffraction

Scanning microbeam X-ray diffraction measurement was performed at BL-4A, Photon Factory. The X-ray beam was focused to 4.5 μm (H) × 3.5 μm (V) at the sample position with Kirkpatrick–Baez mirror and the X-ray wavelength was 0.83 Å or 1.0 Å. We used an X-ray CCD detector (Hamamatsu Photonics Ltd., C4880-50-26A) coupled with an X-ray Image Intensifier (Hamamatsu Photonics Ltd.) [22]. The distance between the sample and the detector was around 180 mm. We scanned a banded spherulite with the X-ray microbeam along its radial direction vertically from the center of the spherulite with a step of 1 μm. Before the WAXD measurement was performed, we continuously irradiated the samples with the X-ray microbeam and confirmed that the sample started to be damaged after the exposure of 100 s. Thus we set the exposure time for each WAXD measurement to be 10 s to avoid the radiation damage. In this experiment, PCL/PVB39 and PCL/PVB48 were used as the sample.

### 2.3. Scanning microbeam small-angle X-ray scattering

Combined measurements of SAXS and WAXD with an X-ray microbeam was performed at BL45XU, SPring-8. The X-ray beam was focused to 12 μm (H) × 5 μm (V) at the sample position by using Fresnel Zone Plate (NTT-AT). An X-ray CCD detector coupled with an X-ray Image Intensifier [22] and a CCD with a fiber optic taper [23] were used for SAXS and WAXD, respectively. We used the WAXD data mainly for the determination of lamellar twisting direction. The X-ray wavelength was 1.2 Å and the distance between the sample and the SAXS detector was around 2300 mm, which was calibrated with the diffraction peak of silver behenate [24]. We scanned a banded spherulite with the X-ray microbeam along its radial direction vertically from the center of the spherulite with a step of 1 μm. Before the SAXS and WAXD measurement, we continuously irradiated the sample with an X-ray microbeam and confirmed that the sample started to be damaged after the exposure of 50 s. Thus the exposure time for SAXS and WAXD measurement was fixed to be 8 s. In this experiment, PCL/PVB39, PCL/PVB45, and PCL/PVB48 were used as the sample. However, the signal-to-noise ratio of WAXD of PCL/PVB48 was not good enough to analyze the detailed twisting manner so that it was not analyzed. In this experiment, the WAXD data were mainly used for the determination of lamellar twisting direction, which could not be determined from only SAXS data. Because only the portion of whole diffraction pattern was detected at the present setting of combined measurements, just the change of integrated diffraction intensity was analyzed and intensity contour maps of WAXD like Fig. 6 were not calculated.

### 2.4. Calculation of the azimuthal distribution of intensity in 110 reflection

To interpret the scanning microbeam WAXD results, we calculated the azimuthal distribution of intensity in 110 reflection in the following manner. We approximated the angular spread of 110 lattice in the reciprocal space with a Gaussian function, the lattice constants of which were $a = 7.97$ Å and $b = 4.76$ Å. We took three independent parameters for the width of Gaussian function, $d_r$, $d_\theta$, $d_\phi$, which are of polar coordinate with the original point O shown in Fig. 2(left). The rotation axis of $\theta$ is $b$-axis, and that of $\phi$ is $a$-axis (see Fig. 2). Then the three-dimensional spread of electron density in reciprocal lattice is represented as below (Eq. (1)).

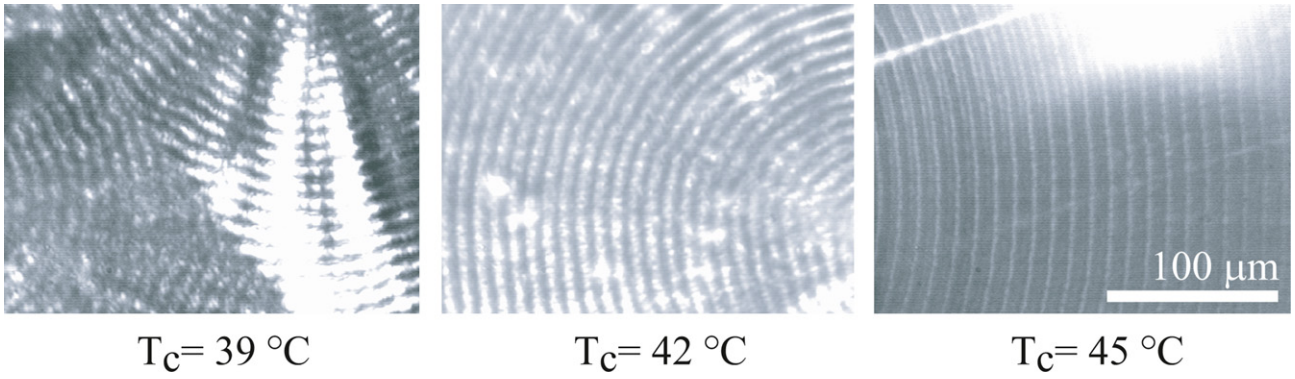


**Fig. 1.** Polarized optical microscope images of PCL/PVB blend crystallized at different crystallization temperatures. The blend ratio of PCL/PVB is 95/5.

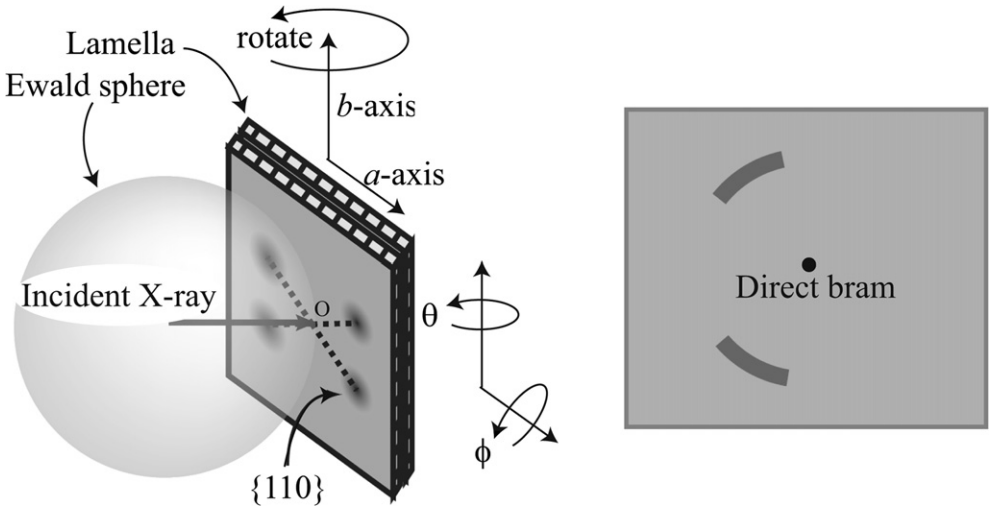


**Fig. 2.** (Left) Schematic view of Ewald sphere and Laue spots in reciprocal space. The cross-section of the sphere shell having $r = \sqrt{(2\pi/a)^2 + (2\pi/b)^2}$ with the Ewald sphere shell yields the azimuthal distribution of 110 reflection (right), where $a$ and $b$ are lattice constants of $a$- and $b$-axis, respectively. The twisting of lamella leads to the rotation of reciprocal space accompanied with the X-ray beam scanning.

$$f(\mathbf{k} = (r,\theta,\phi)) = \exp\left( - \sum_{x=r,\theta,\phi} \frac{(x - x_d)^2}{d_x^2} \right), \quad (1)$$

where ($r_d$, $\theta_d$, $\phi_d$) is a center of Laue point for 110 reflection. This function form was modified from that of Fig. 1 in [21]. Here, $d_r$ relates directly to the degree of crystallinity of packing structure. $d_\theta$ and $d_\phi$ relate to angular spread of packing structure, though they don't have any direct structure correspondences in real space. It should be noted that in Eq. (1) angular spreads of packing structure, $d_\theta$ and $d_\phi$, can be tuned independently from the degree of crystallinity of packing structure, $d_r$, while they could not in the previous paper [21]. The electron density of 110 lattice on the cross-section with the Ewald sphere shell was calculated.

### 2.5. Calculation of the SAXS intensity

A typical SAXS image is shown in Fig. 3 (upper), where a highly oriented pattern is observed. To obtain the structural information, we extracted the azimuthal sector region from the SAXS pattern as shown in the figure and the intensity was azimuthally averaged. After the Lorentz correction, we fitted the intensity profiles with two Gaussian functions which correspond to main- and secondary-lamella peaks as shown in Fig. 3 (lower). It is noted that main lamella has a shorter period than secondary lamella. We, thereafter, call main lamella as short-period lamella, and secondary as long-period lamella.

## 3. Results and discussion

### 3.1. Twisting manner of lamella and packing structure

We observed the twisting manner of lamella with SAXS (in Section 3.1.1) and of packing structure with WAXD (in Section 3.1.2) by rotating the sample. The rotation direction relates to the twisting direction, which is defined by using the handedness of lamellar twisting [20] along the radial direction from the center of the spherulite. We rotated the sample in the two directions: one was the same direction as that of lamellar twisting along the radial direction (phase-retarded rotation), that is, the rotation of sample showed left- (right-) handedness when the lamellar twisting showed left- (right-) handedness. The other was the opposite direction (phase-advanced rotation), in which the sample rotation showed left- (right-) handedness when the lamellar twisting showed right- (left-) handedness. The rotation angle was about 37°.

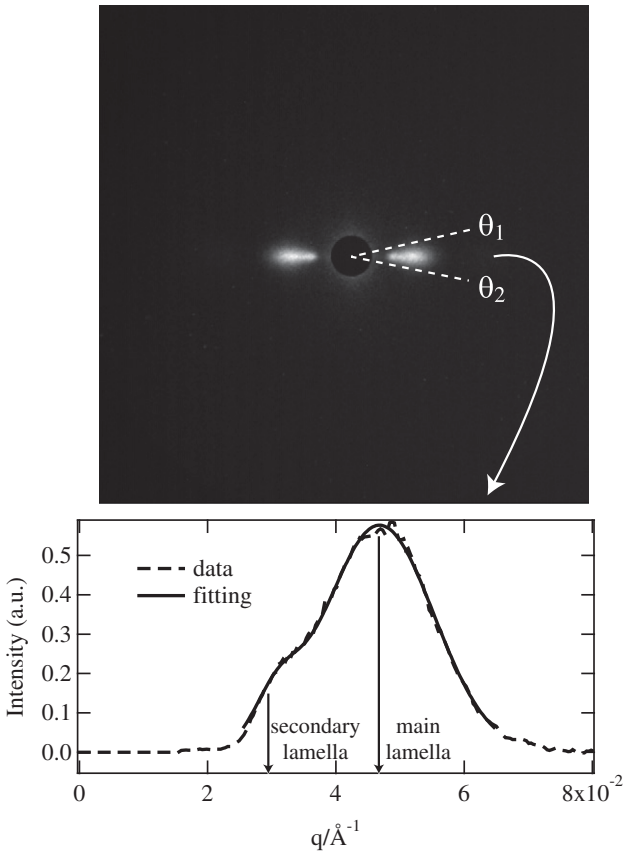


**Fig. 3.** (Upper) SAXS pattern. The white part is where X-ray intensity is high. We extracted the azimuthal angle range from $\theta_1$ to $\theta_2$. (Lower) Extracted intensity profile from Fig. 3 (upper) after Lorentz correction. It is fitted with two Gaussian functions.

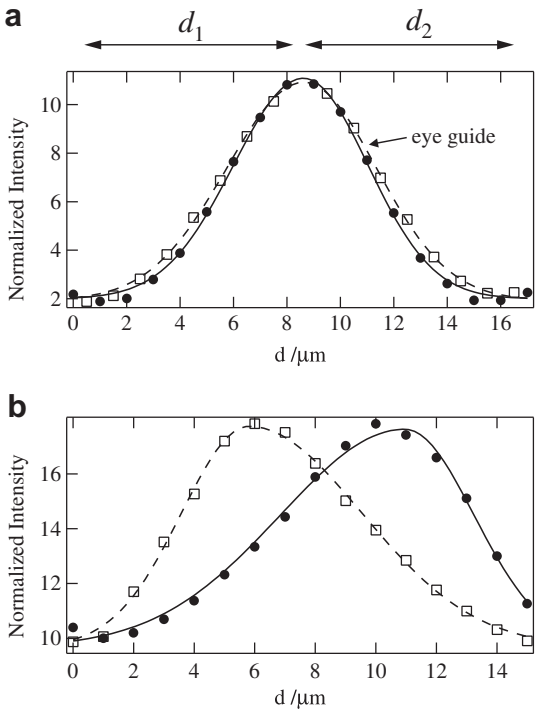


**Fig. 4.** Change of integrated SAXS intensity from short-period lamella during the X-ray microbeam scanning of a period of the banding in a spherulite of PCL/PVB39 (a) and PCL/PVB45, (b). The closed circles and open squares show the results for phase-advanced and phase-retarded rotations, respectively.

### 3.1.1. SAXS results

Fitting results (see Fig. 3) show that the periods of short-period and long-period lamellae are 134 Å and 204 Å, respectively. Fig. 4 shows that integrated SAXS intensity of short-period lamella changes when the X-ray microbeam scans the sample. This change originates from the twisting of short-period lamella. The lamellar twisting leads to a periodic change in SAXS intensity. As shown in Fig. 4, we defined $d_1$ and $d_2$ as the distances from a maximum to the two opposite neighboring minimum points, and used $d_1/d_2$ as a measure for asymmetry of the profile, which relates to the twisting manner. It is clearly shown that $d_1/d_2$ is unity for PCL/PVB39 (see Fig. 4(a)), which means that the lamellar twisting in PCL/PVB39 is uniform. By contrast, $d_1/d_2$ of PCL/PVB45 with the phase-retarded rotation is smaller than unity while that with the phase-advanced rotation is larger (see Fig. 4(b)). This result means that the short-period lamellar twisting in PCL/PVB45 is not uniform and that twisting occurs more tightly in the area of $d_1$ in the phase-retarded plots.

Fig. 5 shows the relation between short- and long-period lamellar twisting for PCL/PVB45. Long-period lamella has the same tendency as short-period lamella in that $d_1/d_2$ is smaller than unity for the phase-retarded rotation while that for the phase-advanced rotation is larger. This result means that the long-period lamella twisting in PCL/PVB45 is not uniform either.

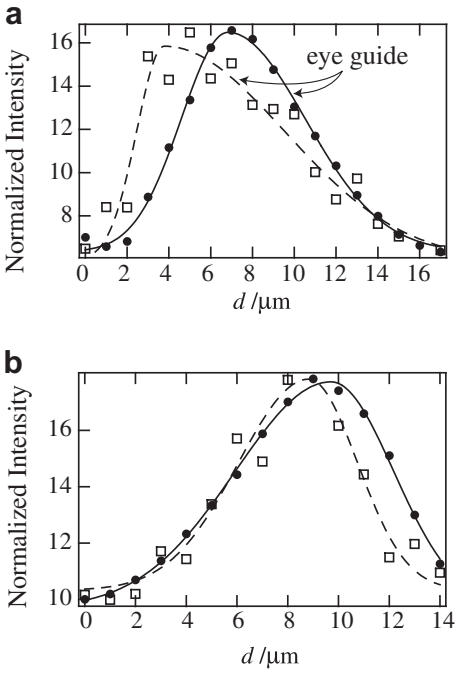


**Fig. 5.** Change of integrated SAXS intensity from short-period lamella (closed circles) and long-period lamella (squares) for PCL/PVB45. The data of short-period lamella are the same as Fig. 4(b). The figures (a) and (b) show the results for phase-retarded and phase-advanced rotation, respectively.

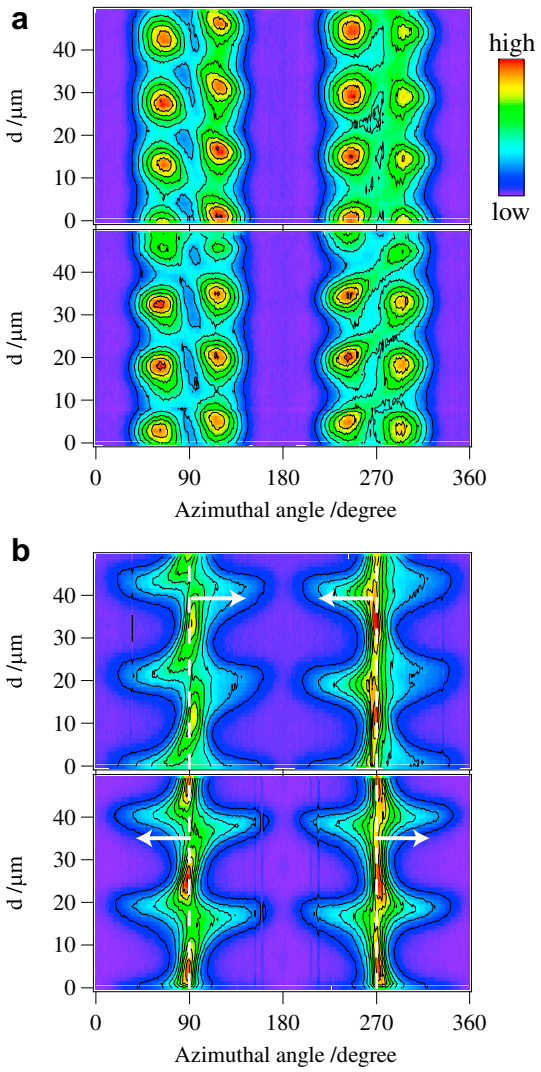


**Fig. 6.** Experimental intensity contour map of 110 reflection for PCL/PVB39 (a) and PCL/PVB48 (b). The upper maps and the lower maps in (a, b) show the results for phase-retarded rotation and phase-advanced rotation of sample, respectively. White-dashed lines show the azimuthal angle of 90° and 270°.

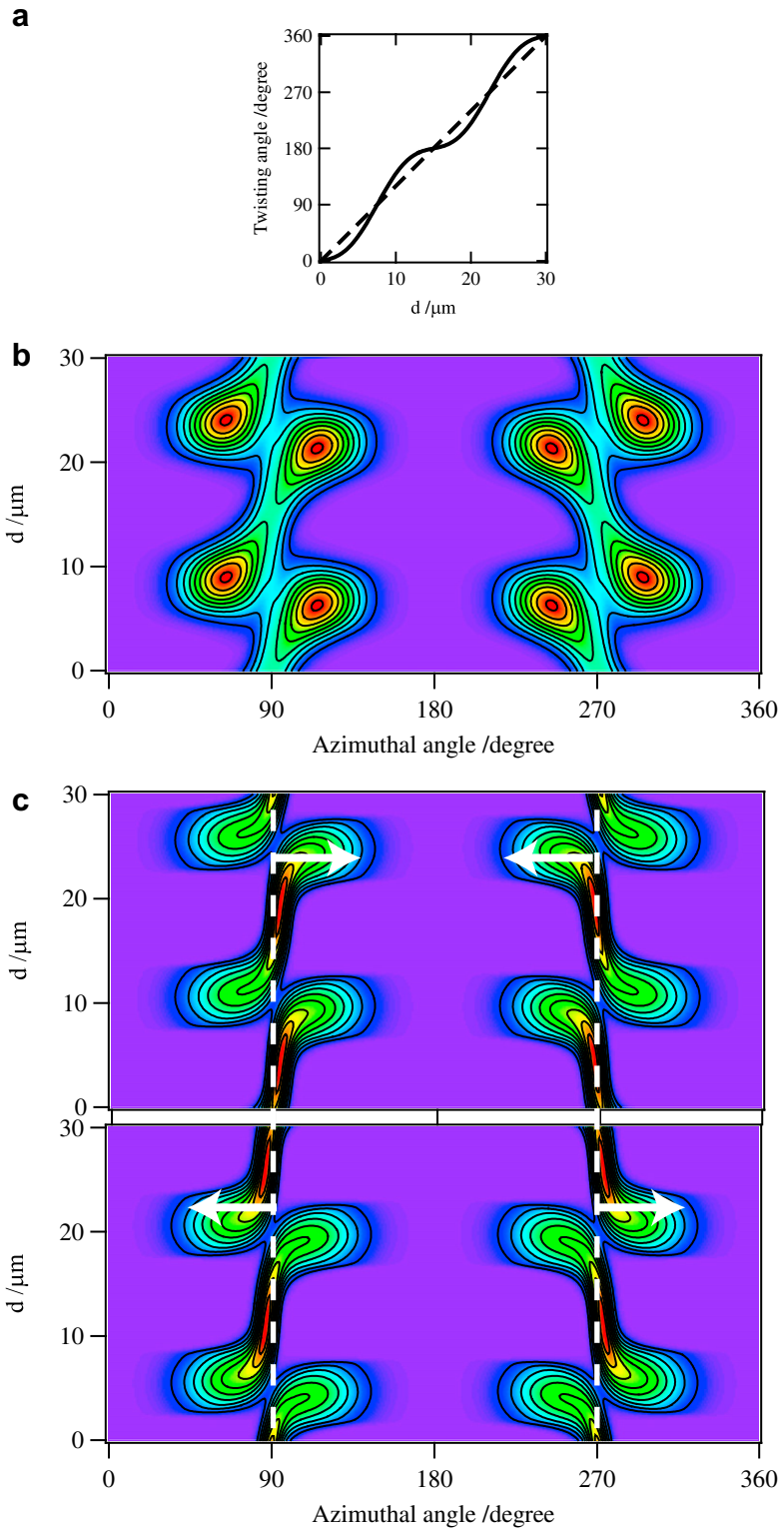


**Fig. 7.** (a) The twisting manner used for calculation. Two lines show lamellar twisting model of step-wise twisting (solid line) and uniform twisting (dashed line), (b) Calculated intensity contour map of 110 reflection azimuthal distribution along the radial direction of spherulite for the uniform twisting of lamella (dashed line in (a)), (c) Calculated intensity contour map of 110 reflection azimuthal distribution along the radial direction of spherulite for the step-wise twisting of lamella (solid line in (a)). The upper and lower figure shows the result for phase-retarded and phase-advanced rotation, respectively. The rotation angle is 40°.

*3.1.2. WAXD results*

In this part, we describe the result of scanning microbeam WAXD in combination with the sample rotation which was performed at BL-4A. Fig. 6 shows the intensity contour map of 110 reflection of PCL/PVB39 and PCL/PVB48. For PCL/PVB39 (Fig. 6(a)), we hardly observed difference in the results between phase-retarded and phase-advanced rotations. On the other hand, there appears a decisive difference for PCL/PVB48 (Fig. 6(b)): the

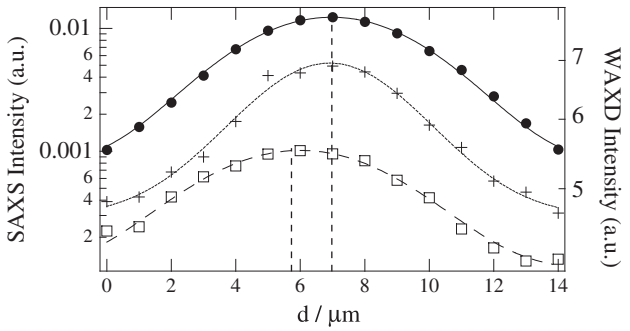


**Fig. 8.** Change of SAXS intensity in a short-period lamella (closed circles) and long-period lamella (open squares) and that of WAXD intensity at azimuthal angle of 90° (crosses) for PCL/PVB45. The intensity peak of each scattering/diffraction is expressed by using lines. There is no phase shift between WAXD intensity and short-period lamella one. In reverse, the phase of long-period lamellar twisting advances by around 15° compared to the other two phases.

azimuthal angle at which the diffraction intensity shows a maximum value shifts by about 3° from 90° to 270° along the white arrows. To interpret the results, we calculated 110 reflection intensity contour maps that are based on the two types of twisting manner as shown in Fig. 7(a). The calculated contour map of twisting at a uniform rate shows no difference between phase-retarded and phase-advanced rotations (Fig. 7(b)). The upper and lower figures in Fig. 7(c) show the contour maps of twisting lamella at a step-wise rate with phase-retarded rotation and phase-advanced rotation, respectively. In this calculation, we found the shift (~3°) along the white arrows in a manner similar to those obtained from the experiment. From the above comparison, we successfully confirmed that the twisting manner of packing structure of PCL/PVB48 are step-wise, while that of PCL/PVB39 are uniform.

Though we tried to measure PCL/PVB45, the measurement failed. This is because the measurement of WAXD with rotation demands enormously accurate experimental setting to avoid sample tilting and extra rotation and we could not accomplish the measurement in the beamtime at synchrotron radiation.

Summing up the Section 3.1, we conclude that the twisting manners of the lamella and the packing structure are the same: they show uniform twisting in the spherulite crystallized at low temperature (around 39 °C) while they show step-wise twisting in the spherulite crystallized at high temperature (around 45–48 °C).

#### *3.1.3. Improvement from previous paper*

In the previous paper [21], we concluded that the twisting manner of lamella, either continuous or discontinuous (step-wise), can be distinguished based on the simulation of intensity contour map of 110 reflection. However, we have noticed that the possibility cannot be excluded that the simulated intensity contour map of 110 reflection would give us ambiguous results, depending on the value of either (1) phase in step-wise twisting or (2) angular spread of packing structure. In the present work, it is confirmed that the ambiguity regarding both (1) and (2) is excluded by employing the rotation of the sample.

### *3.2. Twisting phase relation among short-period, long-period lamellae, and packing structure*

In the above section, we showed that the twisting manner of lamella, whether the continuous twisting or the step-wise twisting, can be determined by analyzing either SAXS or WAXD. In this part, we analyze both SAXS and WAXD to investigate the relationship between twisting phase among three structures; short-period lamella, long-period lamella, and packing structure. Fig. 8 shows the twisting phase relation among three structures for PCL/PVB45. Here the WAXD intensity at an azimuthal angle of 90° is used. At the maximum point of this WAXD data, *c*-axis (001 direction) is normal to the incident X-ray. From Fig. 8, it is clear that the phases of short-period lamellar twisting and packing structure twisting are the same with each other and that they retard compared to that of long-period lamella. The phase shift of twisting angle between long- and short-period lamella is around 15°, which was calculated by using the results that one period of twisting and the interval between the intensity maxima of short- and long-period lamellar twisting is approximately 15 μm and around 1.25 μm, respectively. The fact that the phases of short-period lamellar twisting and packing structure twisting are the same indicates that the *c*-axis of the packing structure is normal to short-period lamella (main lamella), which becomes a key to discuss the origins of the lamellar twisting, while some researchers argue that lamellar twisting happen because *c*-axis is tilted to lamella [25,26]. It is noted that the present result does not mean the *c*-axis in long-period lamella is inclined from the normal of the long-period lamella; the reason is that the intensity of WAXD originating from packing structure in long-period lamella is expected to be too small to be observed, when it is taken into the consideration that integrated SAXS intensity from short-period lamella is one order of magnitude stronger than that from long-period lamella.

Here, we have to admit that this result is inconsistent with that in our previous paper [21], in which we claimed that phase of long-period lamellar twisting retarded compared to short-period one (see Fig. 4 in [21]). This is due to misinterpretation of SAXS data in our previous, which we have found recently. Thus, spatial distribution models of lamella that we discussed in Fig. 9 in [21] somewhat need to be reconsidered.

## 4. Summary

We have developed a scanning microbeam X-ray diffraction technique in combination with the sample rotation so as to determine the lamellar twisting manner in a banded spherulite. With this technique, we have re-confirmed the following two facts without ambiguity which was included in the previous paper [21]:

1. The twisting manner in a banded PCL/PVB spherulite depends on the crystallization temperature.
2. The short-period lamella, long-period one, and packing structure that grow at higher crystallization temperature show step-wise twisting.

Moreover, we observe that the phase of long-period lamellar twisting advances by about 15° compared to that of short-period one, and that *c*-axis of packing structure is normal to lamella, which is represented by dominant short-period lamella, meaning that the packing structure twists with the same phase as lamella.

The present result will be a key to understand the origin of twisting in PCL/PVB spherulite. Furthermore, the scanning microbeam X-ray scattering technique combined with the sample rotation is a powerful tool for the structural analysis of polymer that has micron-scale spatial inhomogeneity, that is, a banded spherulite with twisting lamella.

## Acknowledgements

Prof. A. Iida (KEK-PF) helped us to perform microbeam WAXD at BL-4A. Dr. Y. Sakai (Univ. of Tokyo) helped us to prepare the sample. K. Kamihara, T. Maejima, and Y. Hashimoto (Univ. of Tokyo) supported the X-ray experiments. The experiments at Photon Factory were performed under the approval of the Photon Factory Program Advisory Committee (Proposal No.: 2007G609) and the experiments at SPring-8 were performed under the approval of the SPring-8 Program Advisory Committee (Proposal No.: 2007A1475 and 2007B1153).

## References

[1] Choudhary V, Varma HS, Varma IK. Polymer 1991;32:2534–40.
[2] Lee JC, Nakajima K, Ikehara T, Nishi T. J Appl Polym Sci 1997;65:409–16.
[3] Graebling D, Muller R, Palierne JF. Macromolecules 1993;26:320–9.
[4] Point JJ. Bull Acad R Belg 1955;41:982–90.
[5] Keith HD, Padden FJ. J Polym Sci 1959;39:101–22.
[6] Keller A. J Polym Sci 1959;39:151–73.
[7] Price FP. J Polym Sci 1959;39:139–50.
[8] Gathercole LJ, Keller A, Shah JS. J Microsc 1974;102:95–106.
[9] Keith HD, Padden FJ. Macromolecules 1996;29:7776–86.
[10] Lotz B, Cheng SVD. Polymer 2005;46:577–610.
[11] Toda A, Keller A. Colloid Polym Sci 1993;271:328–42.
[12] Keith HD. Polymer 2001;42:9987–93.
[13] Keith HD, Padden FJ. Polymer 1984;25:28–42.
[14] Luchnikov Valeriy A, Ivanov Dimitri A. J Appl Crystallogr 2009;42:673–80.
[15] Nozue Y, Shinohara Y, Amemiya Y. Polym J 2007;39:1221–37.
[16] Keller A. J Polym Sci 1955;17:351–64.
[17] Calleja FJB, Hay IL, Keller A. Kolloid-Z.Z. Polymere 1966;209(2):128–35.
[18] Gazzano M, Focarete ML, Riekel C, Scandola M. Biomacromolecules 2000;1:604–8.
[19] Gazzano M, Focarete ML, Riekel C, Ripamonti A, Scandola M. Macromol Chem Phys 2001;201:1405–9.
[20] Nozue Y, Hirano S, Kurita R, Kawasaki N, Ueno S, Iida A, et al. Polymer 2004;45:8299–302.
[21] Nozue Y, Kurita R, Hirano S, Kawasaki N, Ueno S, Iida A, et al. Polymer 2003;44:6397–405.
[22] Amemiya Y, Ito K, Yagi N, Asano Y, Wakabayashi K, Ueki T, et al. Rev Sci Instrum 1995;66:2290–4.
[23] Ito K, Fujisawa T, Iwata T. Nucl Instrum Methods Phys Res B 2007;582:673–82.
[24] Blanton TN, Barnes CL, Lelental M. J Appl Crystallogr 2000;33:172–3.
[25] Keith HD, Padden FJ. Polymer 1984;25:28–42.
[26] Silva DSM, Zeng X, Ungar G, Spells SJ. J Macromolecular Sci B 2003; B42:915–27.